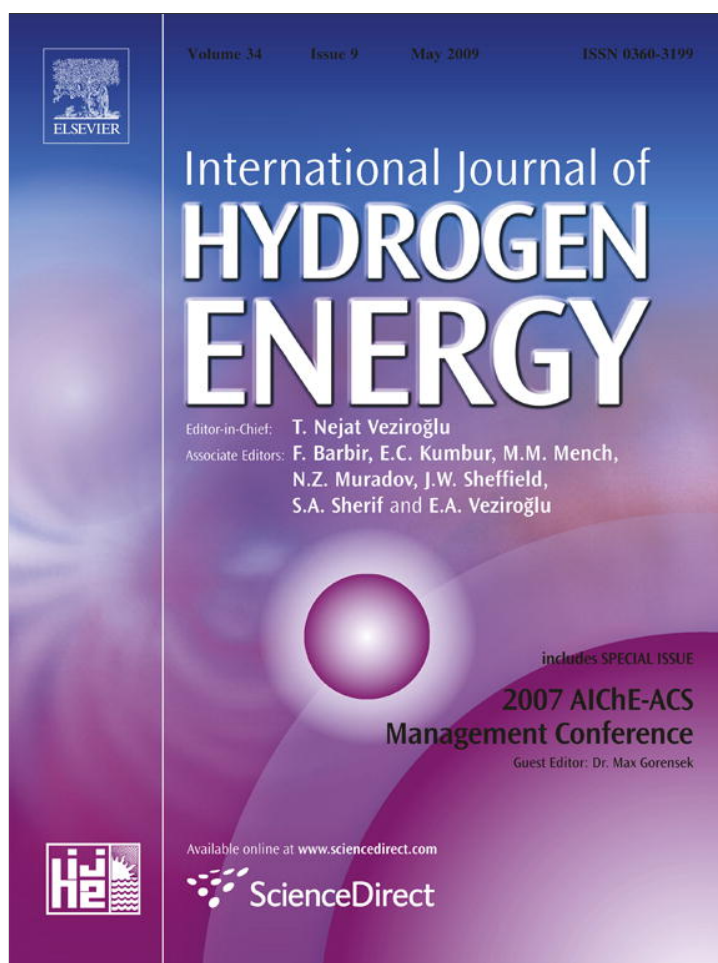


Provided for non-commercial research and education use.
Not for reproduction, distribution or commercial use.

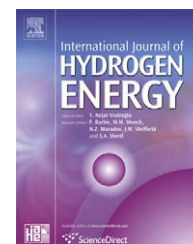


This article appeared in a journal published by Elsevier. The attached copy is furnished to the author for internal non-commercial research and education use, including for instruction at the authors institution and sharing with colleagues.

Other uses, including reproduction and distribution, or selling or licensing copies, or posting to personal, institutional or third party websites are prohibited.

In most cases authors are permitted to post their version of the article (e.g. in Word or Tex form) to their personal website or institutional repository. Authors requiring further information regarding Elsevier's archiving and manuscript policies are encouraged to visit:

<http://www.elsevier.com/copyright>

Available at www.sciencedirect.comjournal homepage: www.elsevier.com/locate/he

Review

Storage of hydrogen in nanostructured carbon materials

Yuda Yürüm^{a,*}, Alpay Taralp^a, T. Nejat Veziroglu^b

^aFaculty of Engineering and Natural Sciences, Sabanci University, Tuzla, Istanbul 34956, Turkey

^bClean Energy Research Institute, University of Miami, Coral Gables, FL 33124, USA

ARTICLE INFO

Article history:

Received 26 February 2009

Accepted 3 March 2009

Available online 26 March 2009

Keywords:

Molecular hydrogen

Hydrogen storage

Carbon nanomaterials

Nanostructured carbon

Physisorption

Chemisorption

ABSTRACT

Recent developments focusing on novel hydrogen storage media have helped to benchmark nanostructured carbon materials as one of the ongoing strategic research areas in science and technology. In particular, certain microporous carbon powders, carbon nanomaterials, and specifically carbon nanotubes stand to deliver unparalleled performance as the next generation of base materials for storing hydrogen. Accordingly, the main goal of this report is to overview the challenges, distinguishing traits, and apparent contradictions of carbon-based hydrogen storage technologies and to emphasize recently developed nanostructured carbon materials that show potential to store hydrogen by physisorption and/or chemisorption mechanisms. Specifically touched upon are newer material preparation methods as well as experimental and theoretical attempts to elucidate, improve or predict hydrogen storage capacities, sorption–desorption kinetics, microscopic uptake mechanisms and temperature–pressure–loading interrelations in nanostructured carbons, particularly microporous powders and carbon nanotubes.

© 2009 International Association for Hydrogen Energy. Published by Elsevier Ltd. All rights reserved.

1. Introduction

Over the next 30 years, two major concerns that are anticipated to become increasingly serious are the decreasing world supply of fossil fuels, particularly those fuels obtained from conveniently extractable sources, and the increasing rate of global warming and climate change, which has closely followed the rising energy demands of society. In efforts to limit the ongoing use of fossil fuels, one attractive strategy has been to develop the technology of “greener” alternative energies to supply power plants, vehicles and most other equipment traditionally run on fossil fuels. In efforts to routinely implement hydrogen, the cleanest burning of all fuels, a major focus has been placed on improving hydrogen manufacture and storage.

Indeed, hydrogen storage is currently the greatest obstacle detracting from the feasible commercial use of hydrogen and as such it appears to have developed into one of the foremost research topics of chemical engineers, chemists, material scientists and all others concerned. Feasible storage modes should be cost-effective and should satisfy the terms stipulated by international environmental and safety laws. On the matter of addressing commercial storage needs, the Department of Energy (DOE) of the United States has targeted the development of adsorbates with a minimum extractable loading of 6.5 wt% hydrogen. In view of this constraint, realizing good hydrogen storage and release performance poses a challenging materials science question. Since hydrogen is gaseous at room temperature and pressure, a plausible mode of storage that continues to receive intensive attention for

* Corresponding author. Tel.: +90 216 483 9512; fax: +90 216 483 9550.

E-mail address: yyurum@sabanciuniv.edu (Y. Yürüm).

0360-3199/\$ – see front matter © 2009 International Association for Hydrogen Energy. Published by Elsevier Ltd. All rights reserved.

doi:10.1016/j.ijhydene.2009.03.001

reasons of practicality and prior track record has been adsorption within microporous activated carbon (AC) powders. Related work has shown that other nanostructured carbons such as carbon nanomaterials and particularly carbon nanotubes (CNTs) can easily and dependably accept and release substantial quantities of hydrogen via physisorption and chemisorption mechanisms. In view of these promising traits, it is not surprising that hydrogen storage using nanostructured carbon materials has quickly defined one of the hottest areas in science and technology. The following text discloses recent highlights of work related to hydrogen storage in nanostructured carbon materials and particularly microporous carbons and carbon nanotubes.

2. Strategies used to achieve hydrogen storage

Three storage techniques examined thus far, amongst others, have included liquefaction, compression and metal hydride formation. Liquefaction and compression strategies have boasted high storage volume efficiencies but they have also brought about high operating costs. In addition, cryogenic liquid hydrogen systems have always experienced bleed-off losses, whereas compressed hydrogen systems have introduced weight and safety concerns relating to hydrogen storage at very high pressures. More closely related to adsorption-based storage have been the metal hydrides. While bearing the potential to load substantial hydrogen, some shortcomings of metal-hydride systems have nonetheless included inadequate hydrogen-loading, high alloy costs, high sensitivity to gaseous impurities, disproportionation, difficulty in achieving initial activation or reactivation, and/or pyrophoricity upon exposure to air [1]. The poor reversibility of hydrogen uptake has marked an additional difficulty that relates to the relatively strong metal-hydride interaction. As a last drawback, metal-hydride systems are known to be heavy. In generalizing to intermetallic or related metal platforms, two factors detracting from ready adoption have been typically low storage capacities and inadequate adsorption-desorption traits, particularly when tested under operational conditions ([3] and references therein, [4,5]). Clearly, a high-capacity hydrogen storage medium is sought to better promote the utility of hydrogen as an energy source, particularly in transport applications, which might use, for example, a hydrogen fuel cell. As implied from the above examples, refinements of several technological aspects are awaited that relate to weight, safety and ease of reversibility, amongst other factors. Hydrogen storage within or along the solid matrices of metals, intermetallics, porous solids and carbon materials appears to feature much potential in addressing the above concerns.

3. Hydrogen storage via adsorption

3.1. Non-carbonaceous adsorbent systems

Of the adsorbent-type metal hydride systems in consideration, magnesium hydride describes one of the most studied

in view of its high hydrogen storage capacity (7.6 wt%), natural abundance and low cost. For comparative purposes, the hydrogen storage capacity of magnesium hydride even exceeds some rare-earth-based hydrides as well as titanium hydride. Despite these promising traits, the high operating temperatures (553–573 K) and slow sorption-desorption kinetics have precluded any wide-spread industrial adoption of magnesium hydride. In efforts to overcome this impasse, many different alloy additives have been assessed for their ability to promote the hydrogen sorption-desorption kinetics of magnesium [161]. Metal particle size has also formed a subject of focus in assessing hydrogenation as it has been proposed that the enthalpy of formation of magnesium hydride decreases once the size of the metallic particle drops below 1 nm [143,145]. Indeed, density functional theory and Hartree-Fock calculations have implied a significant stability change of magnesium versus magnesium hydride as a function of decreasing particle size. In considering other metal-hydride systems, hydrogen release again proved feasible only at unacceptably high temperatures typically spanning 473–1273 K [2]. Of the metal-loaded carbons, variant chemisorption-physisorption strategies under investigation have focused on the chemical storage of hydrogen in organic liquids or related alternative media.

3.2. The merit and challenges of carbon-based adsorbents

Among the previously discussed hydrogen storage techniques, namely compression, liquefaction, metal hydride formation, physisorption and chemisorption, the physisorption of hydrogen along high-surface carbons has defined one focal point in view of the ease of hydrogen uptake and release [57,68]. Among the metal hydrides, metal organic frameworks (MOFs) and carbon materials tested [74–78], the carbon-based materials have received exceptional consideration as potential storage materials in view of their low cost, easy accessibility, good recycling characteristics, low densities, wide diversities of bulk and pore structures, reasonably good chemical stability, and amenability to synthesize variants or post-synthetically engineer traits using a wide range of manufacturing, activation and carbonization methods [79–81]. A range of carbon materials have been proposed, such as CNTs, graphite carbon nanofibers (CNFs), ACs and ordered porous carbons [42,56,82,83]. In transcending from an assortment of porous ACs to the intermediary class of MOFs, hydrogen uptake measurements at 77 K had established that up to 5 wt% and 7.5 wt% hydrogen can be stored in porous carbons and MOFs, respectively [6]. A subsequent disclosure by Chambers et al., which implied that CNFs could physisorb up to 67.55 wt% hydrogen, prompted a remarkable revitalization of research related to potential adsorbents [7]. Amongst the variety of investigations that followed, some entailed the manipulation of carbon materials using metal dopants while others related to the synthesis of high purity carbons of different geometrical structures [8–15]. Despite these efforts, none of the carbon nanomaterials could be made to store hydrogen at a level comparable to the alleged findings of Chambers or the target value specified by the DOE. Similarly, carbon materials had again elicited great expectations

following the results of Dillon et al. [8]. In particular, the account of Dillon inspired a significant and apparently somewhat inconsistently-concluding number of investigations utilizing single-walled CNTs (SWCNTs), multi-walled CNTs (MWCNTs), CNFs and carbon nanohorns (CNHs), which had been prepared using chemical vapor deposition, arc discharge or laser vaporization methods [23–44]. More reliable, self-consistent results have been reported recently with certain CNTs, CNHs and microporous ACs [45–66]. A wide variation of uptake values, ranging from insignificant to large, is depicted herein for the various carbon adsorbents (Table 1).

3.3. Adsorption in carbon-based adsorbents

Adsorptive storage of hydrogen in carbon materials can be viewed as a continuum of two mechanisms, namely, the initial adsorption of hydrogen along the immediate surface of the adsorbent, and the mass transfer and subsequent retention of “internalized” hydrogen molecules within internal spaces of the adsorbent. Adsorption capacity has a composite and complex dependency on several factors including the effectively accessible surface area, the pore size, surface topology, chemical composition of the surface, and the applied pressure and temperature. Of these, two parameters that have been investigated intensively and correlated against the storage of hydrogen are pore structure and specific surface area [42,49] and consequentially many related material techniques have been developed and refined to permit better hydrogen storage within adsorbents [20–22]. From a material design view, the adsorbable quantity has been governed and limited by the adsorbent pore structure, effective pore volume in the narrowest of pores and hydrogen adsorbate density, which reflects the adsorbent-adsorbate interactions. Of the accessible surface, the narrowest of pores has contributed most to hydrogen adsorption. Indeed, micro- and nanoporosity has proven useful in assessing volumetric capacity

whereas mesopores have contributed to the total pore volume, but comparatively very little to storage capacity.

Additional research on high-pressure hydrogen adsorption has proven useful to fully appreciate the advantages of pressure and to ascertain the most suitable adsorbent for a given purpose. Uptake at ambient temperatures and high pressures has often yielded irreproducible and contradictory results. With due consideration to the non-standardized test conditions employed by various groups, these discrepancies have nonetheless underscored the complexity of the adsorbent systems. Many preparative or experimental conditions have caused variations by introducing contaminants or leading to high pressure-induced isothermal variabilities, to name only a few problematic scenarios. In attempting to rationalize the large discrepancy of hydrogen equivalents loaded per gram of carbon nanomaterial, refined measurement techniques and computational studies have been deployed, particularly in the case of carbon nanotubes. Temperature, pressure and mass transfer constraints notwithstanding, the findings verified that part of the difference underscored variabilities of the structure, amount, behavior and homogeneity of the effectively accessible surface. One finding in particular has indicated that porous materials with very narrow pores or pore size distributions are required to improve the storage capacity at relatively low pressures [71,72,73]. For instance, hydrogen storage in SWCNTs appears to have been improved by optimizing the narrow microporosity [142]. On a related note, all attempts to augment hydrogen uptake inside CNTs have failed.

Modeling studies have also contributed to better understanding adsorbent performance. However, while adsorption remains a multi-variable event, most theoretical calculations reported thus far have typically addressed one characteristic of the adsorption event as opposed to examining a selection of parameters and their interrelation. In spite of these limitations, a common finding of the assessments was that hydrogen physisorption alone would be inadequate to meet the DOE specifications at ambient temperature conditions, even under high pressure conditions. For instance, CNTs were explicitly deemed unsuitable as hydrogen carriers for motor vehicle applications. Still, predictions of speedy adsorption-desorption kinetics and comparatively small adsorption enthalpies (<10 kJ/mol) within various porous materials has continued to encourage effects to incorporate a physisorption mode into fast hydrogen recharging applications.

3.4. Physi- and chemisorption contributions in carbon-based adsorbents

Ideally, a composite material that might combine the multi-layer gas-loading propensity of carbon physisorption sites and the reactivity of enthalpically- and kinetically-optimized metal chemisorption sites could give cause to anticipate a high-capacity, readily-reversible hydrogen storage device. In considering the limitations of physisorption, some groups have embraced this combined chemisorption-physorption strategy using either titanium-decorated [143] or nickel-dispersed carbon nanotubes [144] (or fullerenes [145]). To a first approximation, their attempts appeared to surpass the loading capacities offered by physisorption alone [146]. That

Table 1 – Hydrogen uptake values of activated carbons (ACs).

Material	Temperature, K	Loading	Reference
PAN derived ACs	77	2.89–9.67 mmol/g (0.58–1.95 wt%)	[43]
Coconut shell-derived ACs	77	5.85–10.66 mmol/g (1.12.15 wt%)	[43]
CMS T3A	77	1.0 mmol/g	[44]
C molecular sieve Takeda	77	5.5 mmol/g	[44]
Norit AC	77	150 ml (STP)/g	[45]
GS Norit nanofibers AC	77	161 ml (STP)/g	[45]
Carbon A	77	2.3 wt%	[47]
Carbon B	77	2.5 wt%	[47]
Carbon C	77	1.8 wt%	[47]
AC I (Canada)	77	4.5 wt%	[48]
AC	77	25 mmol/g	[49]
CA 1 AC	293	0.65 wt%	[55]
CA2 AC	293	1.59 wt%	[55]
AC F	77	1.0–2.3 wt%	[58]
AX-21 AC	298–233	0.50–0.89	[61]

being said, such attempts have shown drawbacks. While residing far away from the ideal, the long list of potential carbon-supportable chemisorbent agents and their combinations continue to prove attractive in exploring composite material strategies.

For most microporous ACs and related nanostructures, the principal mode of hydrogen storage has pointed to physisorption in view of the rapid hydrogen loading-release kinetics, the complete reversibility of hydrogen sorption, and the consistency of results as referenced against established gaseous adsorbate–adsorbent trends [57,68]. Documented advantages of physisorption over chemisorption have included relatively low operating pressures, relatively low base material costs, simple system designs for storage and an abundance of study models. Thus far, no direct proof has been found to suggest that hydrogen physisorbed along carbon nanostructures could exceed the density of liquid hydrogen under ambient conditions ([3] and references therein).

A common problem in correlating data effectively has been related to inconsistencies of test conditions. Moreover, many approaches have addressed atypical experimental conditions such as high-energy hydrogen atom implantation or unusual simulation parameters such as absolute zero. Even the distinction between physisorption and chemisorption has proved challenging at times, with “intermediate” cases disclosed such as “physisorption” involving strong non-covalent bonds or weak charge transfer. Perhaps the simplest probe to discriminate between physisorption and chemisorption has been enthalpy measurements, as chemisorption typically yields much larger enthalpic changes compared to physisorption. Looking to the kinetics of hydrogen loading and release, physisorption typically reflects much smaller activation energies. Moreover, the observed activation energy is generally a composite value, as it reflects rate-determining events that are linked to physisorption, such as surface transport following contact.

While also subject to discrepancies, theoretical predictions have provided useful insight. Overall, attempts to predict hydrogen absorption capacities or to otherwise elucidate proposed physisorption routes and mechanisms in selected samples have shown variability just as often as consistency. In one detailed theoretical study, the amount of hydrogen adsorbed within aligned bundles comprising square and triangular arrays of SWCNTs was studied as a function of the geometry of the array [16]. The outcome of this work confirmed that the nature of the array could influence hydrogen adsorption. In a related modeling study, a principal question was if hydrogen adsorption would preferentially occur within the core of each CNT or in the space separating aligned CNT bundles. The outcome of these calculations pointed to the latter scenario, with loading being preferred along the outer surface of each tube rather than within the core [17]. The assessment further implied that CNT bundles would have a stabilizing effect on hydrogen adsorption in comparison to individual CNTs. In the same study, three different orientations of the aromatic groups were defined with respect to the CNT axis, forming zigzag, armchair and chiral-type CNT structures. The different arrangements appeared to influence hydrogen adsorption along the CNTs but did not have a bearing on the minute amounts of

internalized hydrogen [17]. In considering the surface topology of CNTs, it was observed that hydrogen adsorption was preferred at specific positions [18]. In particular, density-functional calculations predicted two chemisorption sites at the ends of the tube and one inclusion site within the hollow space of nanotubes. The hydrogen storage capacity within the empty space was also simulated to increase linearly with tube diameter. In another study, Froudakis predicted that hydrogen would adsorb along the tube walls but not enter the tube interior [19]. Binding was simulated to have occurred in “zigzag rings” about the CNT walls, distorting the tube and causing a 15 vol% enlargement. Only after the tube walls became half-loaded with hydrogen did molecular inclusion within the cores become energetically allowed.

3.5. *Physi- and chemisorption kinetics in carbon-based adsorbents*

Apart from the obvious role played by pressure and temperature, the rate of adsorption and release is related to local events occurring immediately preceding, during and following adsorption. The kinetics of adsorption, when governed by physisorption mechanisms, has been characterized by rapid hydrogen uptake and release as well as by complete reversibility. By the very definition of chemisorption, the presence of a catalytic center will profoundly influence the rate of atomization following the initial physisorption of dihydrogen. Similarly, the recombination of hydrogen atoms in the reverse direction can be expected to strongly reflect the nature of the catalytic center. Strong metal–hydrogen bonding has typically given rise to higher reverse activation barriers in chemisorption, necessitating reduced pressures and elevated temperatures to achieve desorption and release. Mechanistically speaking chemisorbed hydrogen species have also been subjected to reorganization at the surface. Quite often, the chemisorbed hydrogen atom is transferred via surface diffusion from the metallic site to a final resting site in the carbon structure. For this reason, the reversal of chemisorption would imply a demanding mechanistic pathway compared to physisorption and indeed chemisorption has been characterized as comparatively sluggish and irreversible, presumably for the reason of added mechanistic complexity.

On a more practical note, the hydrogen adsorption–desorption behavior of CNTs, nanoporous carbon materials and microporous activated ACs have generally displayed marginal-to-zero hysteresis and good adsorption–desorption kinetics at 77 K [45,46]. The very favorable rates have implied an inherent suitability towards fast discharge-recharge applications, albeit the contribution of adsorption enthalpy still remains to be better ascertained under various operational conditions. The precise mechanisms responsible for permitting hydrogen storage in carbon materials have almost certainly displayed structural dependencies that remain to be fully illuminated. What can be surmised from the literature is that carbon materials can store hydrogen at different sites via physi- or chemisorptive mechanisms, and accordingly the microscale storage densities should display some spatial variability [42,49,84–86]. Chemisorption examples are presented in Section 5 following discussions related to physisorption in Section 4.

4. Hydrogen physisorption studies of various carbon-based materials

Developing optimal physisorbents for high-capacity hydrogen storage has essentially addressed three parameters, namely, the intrinsic binding energy between the hydrogen molecule and adsorbent, the accessible adsorption surface, and the bulk density of the adsorbent. The latter two parameters have often defined a composite parameter, i.e., the average surface available per unit volume of the adsorbent. Ideally for any application, the composite parameter should be maximized whereas the intrinsic binding energy should be tailored according to the operating temperature of the hydrogen storage system in question. Many research groups have examined hydrogen physisorption in a vast variety of solid materials [6,87–117]. Carbonaceous materials with optimized structure have typically been investigated at room temperature and 77 K. Of the materials that have defined areas of greater focus, most have been carbonaceous and particularly limited to microporous ACs, AC fibers (ACFs) and amorphous CNTs and SWCNTs. The attractiveness of these base materials has lain in the fact that each could be optimized for hydrogen storage via fine-tunable physicochemical strategies. While displaying consistent trends and behavior, the capacity of such materials has at times proven controversial, test-dependent and/or dissimilar. At elevated temperatures such as room temperature, the storage capacity was found to vary linearly with pressure, while at 77 K the adsorption isotherm of all examples could be satisfactorily explained using the Langmuir model. The surface area and pore size of each material as characterized by nitrogen adsorption at 77 K was further correlated against its respective hydrogen storage capacity to yield a linear relationship between hydrogen uptake and specific surface area for all samples, independent of the nature of the carbon material. With a specific surface area of 2560 m²/g, the highest performing material showed a storage capacity of 4.5 wt% at 77 K [57]. That being said, many scientists have claimed other large storage capacities using different materials [7,9,17,29,39,42,45,125,134–136]. A list of physisorption-based hydrogen loading values are presented in Table 2 for different carbonaceous materials.

4.1. Microporous activated carbons

Well-developed microporous materials have an established history as storage media. The hydrogen adsorption capacity of different microporous ACs predictably reflects pore structure parameters such as specific surface area, micropore surface area, total pore volume and micropore volume. In view of the rapid adsorption–desorption kinetics and almost perfect reversibility traits of ACs, physisorption-based hydrogen storage investigations have attracted much interest. The hydrogen storage capacity of these materials has appeared proportional to the specific surface area and micropore volumes. Narrow micropores were found to preferentially load hydrogen, implying the predominant role of physisorption. While boasting a long-term track record in the adsorption of other gases, ACs have nonetheless been plagued

with conflicting experimental and theoretical results for hydrogen adsorption.

Unlike CNTs, the major disadvantage in correlating experimental and theoretical efforts has been the enormous chemical and structural complexity and heterogeneity of ACs. Experimental findings [24,57,69,115] have yielded adsorption values in the range of 0.5–5.5 wt%, with a marked dependency on the solid employed. Still, the highest of loadings have measured below 1 wt% at 100 bar and 298 K, even in cases with highly developed pore structures approaching 2800 m²/g as specific surface area [82]. Likewise, theoretical work has yielded predictions ranging from 0.03–23.8 wt% in well-defined models [92,116,117]. Some theoretical research has indicated that the proposed DOE threshold of 6.5 wt% cannot be realized [105–114] whereas another comprehensive treatment has revealed that microporous carbons are the only materials, which might permit 6.5 wt% hydrogen loading as targeted by the DOE [159]. In the latter work, the results implied that adsorbed gases should display greater densities than the respective density of the liquefied gas [28,143,147–160]. It was further proposed that the accumulation of dihydrogen within porous carbons had reflected an unusual organization of hydrogen arrayed within the pores. Gadiou et al. prepared ordered microporous carbonaceous solids and observed hydrogen densities of up to 0.1 g/cm³ within the pores, which in absolute terms exceeded the density of liquid hydrogen (0.071 g/cm³) [58]. Amongst the most current theoretical work, Georgakis et al. has forecast the hydrogen loading of microporous carbonaceous solid models and oxygenated microporous carbonaceous solids at 77 K [92]. Predictions varied from between 0.7–4.4 wt% and 0.2–3.3 wt% in basic and oxygenated models, respectively, in response to the pore size of the materials. Georgakis et al. further suggested that matrix-loaded hydrogen could indeed exceed the density of liquid hydrogen [92]. The majority of experiments have demonstrated that loadings of about 2.5 wt% at low pressures (1–10 atm) [42,69] and 5.5 wt% at high pressures (up to 60 atm) [24,57] were attainable. Georgiev et al. studied hydrogen adsorption on high purity chemically-activated ACs, both experimentally and theoretically, near the triple point [87]. An adsorption maximum of 4 wt% was noted under these conditions, whereas hydrogen adsorption was virtually absent at room temperature. A threshold micropore size of 0.6 nm was reported as the starting point of hydrogen adsorption. Thomas concluded that hydrogen adsorption on microporous carbons can reach 5 wt% at 77 K, but only 0.5 wt% at ambient temperatures and high pressures [6]. In comparison, thermodynamic surveys have implied adsorption values ranging from 0.03 to 1.90 wt% for a stack of graphitic sheets [154] or 0.05 to 2.25 wt% for isolated sheets [148], and 23.8 wt% depicting the upper limit for porous carbonaceous and oxygenated carbonaceous models at high pressures (80 MPa) [117,155]. A super AC, Maxsorb, showed the best hydrogen storage capacity of 0.67 wt% at room temperature. Lowering the temperature to 77 K gave rise to a significant increase of the hydrogen storage capacity as Maxsorb adsorbed 5.7 wt% hydrogen at 77 K and 3 MPa hydrogen pressure. The final results also implied that it would be difficult to meet the DOE target of 6.5 wt% by physisorption alone, even at 77 K. Still, other investigators have experimentally and

Table 2 – Physisorption-based hydrogen uptake values of carbonaceous materials.

Type of carbonaceous material	Temperature, K	Pressure, MPa	Hydrogen uptake, w/w %	Approach	Reference
Super activated carbon	93–293	79.4	23.8	Theoretical	[112]
Microporous activated carbons	77	0.1–1	0.03–23.8	Theoretical	[87]
CNTs and SWCNTs	298–395	9–14	0.3–20.0	Theoretical/ Experimental	[6,7,9,88–108]
GNFs	300	8	10–15	Experimental	[40,120]
CNTs	298	10	>10	Experimental	[130]
CNTs	115	3	9.2	Experimental	[85]
SWCNTs and MWCNTs	77	10	5–8	Experimental	[9,55,118,125]
SWCNT/C60 Fullerene	300	1000	7.7	Theoretical	[86]
Porous carbon	77	0.1	0.5–7.5	Experimental	[4]
GNFs	293	12	6.5	Experimental	[35]
MWCNTs	100–300	15	6.3	Experimental	[111]
Microporous activated carbons	20–298	0.1–100	0.5–5.5	Experimental	[22,55,67,110]
MOFs	77	0.1	5	Experimental	[4]
SWCNTs	298	10	4–5	Experimental	[7]
MWCNTs	293	13.5	4.6	Experimental	[32]
Pretreated SWCNTs	298	10	2.4–4.2	Experimental	[7]
Heat treated MWCNTs	298	10	1.3–4.0	Experimental	[24]
High purity chemically activated carbons	13.8	0.007	4	Theoretical/ Experimental	[82]
MWCNTs	298	1–10	4	Experimental	[27]
High purity chemically activated carbons	298	1–2	<4	Theoretical/ Experimental	[82]
Microporous activated carbons, oxygenated	77	0.1–1	0.2–3.3	Theoretical	[87]
ACs and SWCNTs	77	0.1–1	2.5–3	Theoretical	[67]
Graphitic carbons	100–200	0.5	0.09–1.1	Theoretical	[111]
Activated carbons	298	10	1	Theoretical	[77]
SWCNTs and MWCNTs	298	10	<1	Experimental	[55,66,87,118–128]
SWCNTs, MWCNTs and GNFs	293	10	<1	Experimental	[15,129–131]

theoretically professed high hydrogen storage values in carbon materials via physisorption. Clearly, the large disparities amongst various theoretical predictions and experimental results for hydrogen adsorption on microporous ACs remain to be elucidated.

4.2. Carbon nanotubes

CNTs, which define a relatively new class of carbonaceous materials, have become a source of much academic interest. After the discovery of CNTs by Iijima in 1991, the capacity of CNTs to store hydrogen has fascinated many scientists [118]. In the case of SWCNTs, hydrogen adsorption has strongly reflected sample preparation, as shown by some notably different hydrogen loadings. In spite of high cost issues, SWCNTs have appeared to outperform ACs, at least in some respects, as evidenced by a higher hydrogen coverage per unit area. The larger bulk density of SWCNTs has also enhanced volumetric storage [69] and experimentally and theoretically obtained hydrogen loadings have ranged between 0.3 and 20 wt% in such materials [8,9,93–113]. The major advantage of CNTs is related to the fact that the carbon structure is

practically known. This aspect has permitted the correlation of experimental data with theoretical predictions and has served to better illuminate the storage mechanism. That being said, one aspect that continues to detract from better modeling the behavior of CNTs is related to metallic impurities, which invariably become incorporated into the structure of CNTs during production. The spatial distribution and chemisorptive effects of such metals are not only subject to variability, but their presence can also influence the adsorption mode and capacity.

Ye et al. have proposed a nanocontainer for the storage of hydrogen, comprising a SWCNT with two C60 fullerenes embedded within the inner core to work as tiny trap/release valves [91]. Using molecular dynamics simulations, the group was able to predict a maximum hydrogen adsorption capacity of 7.7 wt% at pressures greater than 10,000 bar. Even here, measurements have been the subject of debate, as a different group reported that CNTs posed no benefits when compared against ACs for hydrogen storage [90]. In fact, a maximum hydrogen adsorption of 9.2 wt% was attained in their work when assessing slit-shaped pores in the ACs. An optimal adsorption temperature of 115 K was suggested.

Dillon et al. described substantial hydrogen adsorption in SWCNTs at ambient temperatures, causing a turn in research in the direction of such materials [8]. The gravimetric storage density of a low-purity SWCNT sample ranged from between 5 and 10 wt%. The hydrogen storage capacity of various carbon nanostructures, including SWCNTs [8,9,11,41,119,120,121], MWCNTs [68,122,123], graphite nanofibers (GNF) [7,45,46,125,126], and other nanocarbon materials [41], together with the conventional microporous ACs [41,46,126], have been extensively explored experimentally and theoretically after the report by Dillon et al. [8]. The majority of results indicated that the storage capacity of SWCNTs and MWCNTs for hydrogen was lower than 1 wt% at ambient temperature and about 10 MPa [57,68, 92,123–133] but the capacity could be raised considerably to between 5 and 8 wt% when decreasing the temperature of adsorption to 77 K [11,57,123,130]. Still, other theoretical assessments of hydrogen adsorption on CNTs implied that the 6.5 wt% threshold specified by the DOE could not be achieved [16,100,136–140,148].

Liu et al. [9] reported 2.4–4.2 wt% hydrogen storage at room temperature and 10 MPa, with pretreated SWCNT samples. Liu et al. further claimed 4–5 wt% adsorption in SWCNTs at 100 atm and room temperature [9], whilst Ye et al. determined a H/C ratio of about 1/1 for hydrogen on SWCNTs at 80 K [11]. Results for hydrogen adsorption on MWCNTs provided values of 2.0 wt% (40 bar) [113], 3.7 wt% (69 bar) [114], 4.0 wt% (100 bar) [29] and 6.3 wt% (148 bar) [116]. Li et al. showed that the structure and crystallinity of MWCNTs had affected the hydrogen storage capacity, as exemplified by an increase from 1.3 to 4.0 wt% after heat-treatment at 2473 K [26]. Hou et al. examined hydrogen storage in MWCNTs and correlated the capacity against the average outer diameters, reporting a maximum value of 4.6 wt% at 293 K and 13.5 MPa [34]. As anticipated, the hydrogen storage capacity was found to vary linearly as a function of the diameters of the MWCNT. Hou et al. further claimed that small “carbon islands” might have served as major hydrogen adsorption zones in these MWCNTs [34]. In contrast, Tibbetts and Meisner, and Shiraishi et al. reported a 0.3 wt% capacity [79,140]. More strikingly, they proposed that any claim stating adsorption values higher than 1 wt% had arisen from experimental inaccuracy.

In fact, hydrogen loadings achieved by physisorption were found to not exceed 1 wt% when quantified using ion beam analysis.

4.3. Metal-organic frameworks

MOFs can display extremely high surface areas as well as favorable adsorbate-surface interactions, and as such they have attracted much interest for their potential merit as storage media. Strategies to yield MOFs with enhanced hydrogen adsorption capacity, more favorable adsorption enthalpies and better kinetic confinement characteristics continue to be tested. The nature of MOFs is such that the low pressure zone of hydrogen adsorption isotherms has appeared primarily dependent on the adsorbate-adsorbent interaction, whereas other factors would grow increasingly important in proceeding to higher pressures ([3] and references therein). This claim has been supported experimentally for MOFs (and *in silico* for carbon nanostructures) ([3] and

references therein). Despite BASF's commendable hydrogen-powered car campaign, hydrogen physisorption on MOFs (and undoped carbon nanostructures) currently remains below the DOE-assigned feasibility target to utilize hydrogen as a transportation fuel in motor vehicles. Hence, the scope of MOF-promoted adsorption technologies appears limited for the time being to specific applications, such as the bulk storage of hydrogen [70]. Presently, an upper limit of 7.5 wt% hydrogen adsorption has been noted for MOFs under conditions of high pressure, whereas 5 wt% adsorbed hydrogen has been observed on microporous ACs at 77 K under comparable conditions [6]. The temperature dependence of hydrogen adsorption in MOFs is clearly an important parameter in assessing storage performance and purpose. Like the ACs, there has been no basis to anticipate that raising the pressure alone should enhance room-temperature adsorption to a level comparable at 77 K. Still, kinetic trapping/confinement of hydrogen has been observed in some MOFs. This finding has implied a potential mode of entrapment that could lead to materials displaying better temperature-dependent hydrogen adsorption traits [6]. Thus, optimizing the surface area, topology and reactivity, and fine-tuning such entrapment kinetics by tweaking framework flexibility and pore-opening dynamics describe some ongoing themes of research in MOF chemistry.

4.4. Graphite nanofibers, carbon nanohorns and graphitic carbon inverse opal

GNFs consist of graphene sheets arranged in a parallel, perpendicular, or angular orientation with respect to the fiber axis, with only the graphene edges exposed. It has been professed that the unique layering structure of GNFs can serve to intercalate multiple layers of hydrogen. Indeed, some unexpectedly high hydrogen storage capacities in GNFs have been claimed by Chambers et al. [7]. In particular, the GNFs tested appeared to adsorb more than 20 L of hydrogen per gram at 298 K and 12 MPa. High, reversible adsorption values in GNFs have also been witnessed by Gupta and Srivastava [42,125]. Some findings were as great as 10–15 wt% at 300 K and 8 MPa. Browning et al. indicated that GNFs had adsorbed up to 6.5 wt% at 12 MPa pressure and ambient temperature [37]. In direct contrast, Monte Carlo simulations with chemisorption modes deliberately precluded yielded less than 1 wt% hydrogen storage at room temperature and 10 MPa in various carbon materials such as GNFs, SWCNTs and MWCNTs [17,134–136]. The juxtapositioning of these findings strongly implied a chemisorption contribution to hydrogen loading, which could indeed apply in view that GNFs are typically prepared in the presence of high amounts of metal catalyst.

On a related study, Cao et al. reported that “graphitic carbon inverse opal” (GCIO), a new class of microporous carbon material, could serve as an exceptional absorbent for hydrogen storage at room temperature [137–139]. In GCIOs, the optimum pore diameter for adsorbing hydrogen was found to be approximately 0.7 nm, which would correspond to the dimensions of a double layer [138].

In 1999, Iijima et al. prepared a new carbon particle via carbon dioxide laser ablation of graphite at room temperature [167]. The catalyst-free particle comprised an aggregate of

numerous horn-shaped, single-walled graphene “sheaths”, thus qualifying the term single-walled CNHs (SWCNHs). The SWCNHs so prepared appeared to share similarities to SWCNTs. However, in view of the pure (>95%) and essentially metal-free composition, SWCNHs have been deemed as ideal models to study hydrogen storage via physisorption.

5. Hydrogen chemisorption studies of various carbon-based materials

Developing optimal carbon-based chemisorbents for high-capacity hydrogen storage has essentially addressed the need to prepare readily reversible storage systems as well as to better understand the interplay of catalytic metal sites and the unsaturated carbon matrix. The intrinsic binding energy between the hydrogen molecule and adsorbent, the accessible adsorption surface, and the bulk density of the adsorbent have once again played a role, but the interrelationships of such parameters overall has proved more complex in comparison to cases involving physisorption. It has been generally professed that metallic compounds chemisorb hydrogen atoms via dissociation of dihydrogen whereas carbon materials physisorb hydrogen molecules by establishing weak van der Waals interactions. The two storage modes have illuminated two very different scenarios as atomic hydrogen typically locates, at least initially, within interstitial bulk sites of intermetallic compounds, whereas dihydrogen molecules should adsorb along the surface or within the pores of carbon materials. In combining these physisorption and chemisorption modes, composite storage materials comprising metal dopants and carbonaceous supports have shown a propensity to display the advantages of both. The hydrogen storage capacity of various metal-bearing carbon materials has been summarized in several reports [24,94,127,163–166].

5.1. Mesoporous carbons

Following the discovery of ordered mesoporous carbons by Ryoo and co-workers [183], template-based syntheses of carbonaceous materials have evolved into a well-defined and pivotal area in carbon-metal composites research [184–189]. In keeping with this theme, Campesi et al. studied carbon templates bearing either intermetallic compounds or hydride forming metals (e.g. Pd) in hopes to develop materials with improved hydrogen storage properties as well as to confirm the positive professed effect of small-size metal clusters [182]. In a related work, the storage capacity of Pd-doped ordered mesoporous carbons was measured, with the 10 wt% metal component homogeneously distributed as 2 nm clusters [183]. Palladium did not affect the hydrogen storage capacity when compared to undoped samples at 77 K and 1.6 MPa, as the uptake of hydrogen was attributed to physisorption along carbon under those conditions. At room temperature and moderate pressures (0.5 MPa), however, the same doped samples yielded an eight-fold improvement over the corresponding Pd-free carbon templates. Additional work has confirmed that this notable increase of hydrogen uptake underlined the contribution of chemisorption originating at the Pd clusters. Metal-carbon interfaces of metal-doped

activated carbon samples has been quantitatively examined by Lueking and Yang [12] and Yang et al. [175] in the course of establishing a relationship between spill-over source and the receptor that controls spill-over. As a result of their work, it has been confirmed that metal particles, as dopants, do present an effective hydrogen adsorption and spill-over mechanism.

In addition to ion radiation, carbon surfaces have also been oxidatively re-functionalized using oxygen, nitric acid or other oxidants to yield oxygen-containing surface-pendent functional groups. Gas phase-oxidized activated carbons showed a rise in hydrogen adsorption at temperatures between 400–700 °C [168]. Conversely, liquid-phase persulfate-oxidized activated carbons displayed a loss of hydrogen adsorption capacity [169]. Chemisorption-mediated hydrogen uptake values are presented in Table 3, reflecting the different classes of carbonaceous materials.

5.2. Carbon nanotubes

As noted in the previous sections, the hydrogen storage capacity of CNTs can differ extensively. The basis for such a difference is neither obvious, nor is it likely related to one particular reason. Common explanations include differential activation by the presence of varying amounts and types of impurities within the samples (i.e., metal catalysts, amorphous carbon), as well as different processing histories and pretreatment procedures prior to conducting the adsorption experiments. Currently it is not precisely clear how these metallic catalyst particles, which are used throughout the synthesis of nanotube samples, might be influencing the hydrogen storage capacity of CNTs.

Among the newer of results, hydrogen adsorption in bundles of alkali metal-intercalated CNTs has been reported by Simonyan and Johnson [164]. Overall, hydrogen adsorption in metal-intercalated CNT bundles was substantially enhanced in comparison to unmodified CNTs. The size and charge of these metal clusters were further elucidated using a simple model. Electronic charge transfer from the metal clusters to the nanotubes was also modeled. Hydrogen adsorption in CNT bundles was simulated as a function of various lattice spacings and correlated against related experimental results, which depicted swelling of nanotube bundles upon hydrogen loading. Good agreement was found between theory and experiment at higher pressures. Thus it could be said that hydrogen at 77 K very likely intercalated and swelled the nanotube bundles, increasing the adsorption capacity in the process.

Currently, most theoretical studies have strived to estimate the hydrogenation properties of hybrid carbon/metal compounds. Yildirim and co-workers [143,145] have studied the interaction between hydrogen molecules and Ti-doped SWCNTs using *ab initio* calculations. From their computations, they estimated a maximum hydrogen uptake of 8 wt%. Interestingly, the computations implied that a naked Ti atom should coordinate to dihydrogen without any energy barrier. The Ti-H₂ entity thus formed was further complexed to three additional H₂ molecules, yielding a Ti-4H₂ system. These calculations have corroborated experimental findings in the sense that decreasing the size of metallic clusters served to

Table 3 – Chemisorption-facilitated hydrogen uptake values of carbonaceous materials.

Type of carbonaceous material	Incorporated material or process used	Temperature, K	Pressure, MPa	Hydrogen uptake, w/w %	Approach	Reference
CNTs	Li, K	298–673	–	14–20	Experimental	[11]
CNTs and fullerene	Li, Ti, Sc, Ni, V, Pt, Pd	298	0.1	9	Theoretical	[165,166]
SWCNTs	Ti	–	–	8	Theoretical	[152,154]
CNMs	Mg	363–453	0.5	5–7.6	Experimental	[156]
CNTs	B, Pd, Pt	300	8	0.5–3.7	Theoretical/ Experimental	[10,170,173]
CNTs	Alkali metals	80	12	2	Theoretical	[159]
Surface modified ACFs	Ni	303	10	1–1.6	Experimental	[84]
CNTs	Ion irradiation	–	–	1	Experimental	[187]
SWCNTs and activated carbons	Pd	298	9	0.7	Experimental	[172]
CNTs	Pd, V	298	2	0.66–0.69	Experimental	[175]
CNTs	Pd	298	1.67–2.2	0.35	Experimental	[176]
CNTs	K	–	–	5 H ₂ /K	Theoretical	[99]
Ordered mesoporous carbons	Pd	77	0.5–1.6	0.78 H/Pd	Experimental	[177]
Graphene sheets and SWCNTs	Pt	298	–	1.4 H/Pt	Theoretical	[185]
Activated carbons	Oxidation	78	4	–	Experimental	[163]

noticeably alter the thermodynamics of hydrogen absorption. Similarly, the enthalpy change of magnesium hydride as a function of nanosize was confirmed by the recent work of Rud et al. [161]. The group specifically determined that the crystallite size and lattice strains of a Mg–carbon nanomaterial (CNM) composite was less than in magnesium–graphite and magnesium–graphite–nickel powders. Not surprisingly, a sample of Mg–carbon nanomaterial composite displayed better hydrogen sorption kinetics than the corresponding magnesium–graphite and magnesium–graphite–nickel samples. At 453 K, ~5 wt% of hydrogen could be stored within the Mg–CNM composite. Hydrogen sorption was observed to commence at temperatures as low as 363 K. Boron-substituted nanotubes (BCNTs) have also depicted a potential technology base with ideal prospects [178]. Template-assisted syntheses of BCNTs were achieved via the carbonization of hydroborane polymers encased within an alumina-based membrane as template [178]. Such work has yielded BCNTs that feature an impressive 2 wt% hydrogen capacity at 80 bar and 300 K.

In other studies, research groups have assessed the effects of lithium or potassium inclusion on the chemisorptive behavior of CNTs, realizing improvements in many cases. For instance, Chen et al. observed that lithium and potassium-doped CNTs had yielded considerably improved hydrogen capacities, with loadings increasing from 14 to 20 wt% as temperature was incrementally lowered from 400 °C to ambient [13]. They further proposed that a chemical dissociation had occurred inside the nanotubes and their work led to various investigations [15,41,52,120,123–128], which created some controversy, as expressed by Ding et al. [102].

Transition metal-doped CNTs, with s–p–d hybridization states involved, have served to intrigue and to impress in view of high storage measurements [170,171]. Despite this attractive finding, the storage attributes of these complex systems

have not been elucidated, which perhaps explains why transition metal–CNTs continue to define the most intensively studied of dopant-facilitated carbonaceous storage systems [12,175,177]. The hydrogen bonding attributes and orbital geometries of Ti, Sc, Pt, and Pd dispersed on CNTs (or fullerene and other aromatic hydrocarbons) have been assessed using density functional calculations and found to reinforce the notable increases of hydrogen storage capacity [170,171]. In particular, an unusual hybridization state has been found to permit a direct bond between molecular hydrogen and the metal center through what has become known as Kubas's interaction, after the innovative work of Kubas [172]. A key factor in stabilizing such Kubas-type complexes has been the contribution of vacant metal *d*-orbitals of suitable energy [172,173]. The precise hydrogen-loading mechanism of CNTs (as well as other metal-bearing carbon-based materials) has been rationalized. In CNTs, metal atoms residing within the composite have been envisaged to facilitate the transfer of molecular and atomic hydrogen onto various binding sites via a spill-over mechanism [12,174–177]. For instance, Reddy and Ramaprabhu recently deposited 3–5 nm nanocrystalline platinum dispersions along SWCNT surfaces [179]. In conducting this work, they noted that Pt had enhanced hydrogen storage by dissociating dihydrogen and thereby providing a means for atomic hydrogen to strongly adsorb at the defect sites of each nanotube. Ansón et al. suggested that SWCNTs (and activated carbons) bearing palladium nanoparticles could store 35% more hydrogen via an apparent spill-over mechanism [177]. As a last example, Pd-doped CNT systems featured an estimated 3.7 wt% hydrogen storage capacity when 50% of the hexagons in the (8,0) SWCNT had become occupied by Pd atoms [177]. Interestingly, many experimentally measured Pd–CNT systems tested comparatively low (~0.5 wt%), with a marked dependency on the test conditions [12,174,177,178]. A part of this discrepancy was related to the inadequacy of

metal–nanotube interfaces, which have been professed to impede high loadings in metal-doped CNTs [12,175].

Zacharia et al. explored the room-temperature hydrogen storage capacities of Pd- and V-doped CNTs at 2 MPa using a Sieverts apparatus [180]. The storage capacity was determined as 0.66 and 0.69 wt%, respectively, which depicted a near 30% increase in comparison to the undoped CNTs. Furthermore, these transition metal-doped CNTs displayed rapid initial adsorption kinetics in comparison to the base carbon materials. Once again it appeared that these catalysts had increased the storage capacity by means of a spill-over mechanism. Attempts to re-load previously loaded CNTs implied that virtually 70–85% of the spilled hydrogen was located at physisorption binding sites such as external walls or groove sites.

Pd-doped CNTs prepared by either impregnation or *in situ* condensed-phase reduction have also been studied using the Sievert volumetric apparatus [181]. The doped samples displayed almost twice the hydrogen storage capacity of undoped samples at 298 K and 1.67–2.2 MPa. In particular, adsorption experiments conducted at 298 K and 2.2 MPa yielded a maximum of 0.35 wt% hydrogen storage. Interestingly, any potential contribution of spill-over effects in these samples appeared to have been precluded, as the majority of metal particles lay buried within the nanotube channels. Hence, dissociative chemisorption and spill-over were clearly retarded by poor access and positioning. In addition, the release characteristics did not show a significant bearing on the choice of method used to dope these CNTs. Instead, the amount liberated depended mainly on the storage capacities of the CNTs. Simply mixing CNTs with palladium catalyst tripled the hydrogen uptake. That being said, the loading capacity of each undoped support remained the predominant factor in determining the overall uptake of catalyst-carbon mixtures. Henry-type adsorption characteristics further implied that significant adsorbate–adsorbate interactions did not exist in the experimental pressure regime [180].

Lastly, the introduction of structural defects via ion irradiation has presented a potential alternative approach to improve hydrogen adsorption and specifically to enhance chemisorption of hydrogen in CNTs [192]. In this work, SWCNTs were irradiated using a hydride beam with a gun potential of 13.5 keV, yielding defect sites that could presumably enhance hydrogen adsorption. Desorption measurements conclusively showed that post-irradiated, hydrogen-loaded samples had liberated more hydrogen than pre-irradiated, hydrogen-loaded samples. As well, CNT films have been hydrogenated using ion beam implantation of atomic hydrogen. The C–H bonds formed were shown to be stable at ambient temperature and quantitatively cleaved at 600 °C, thereby establishing the reversibility of hydrogenation and potential merit of the material. These results, more than any other, drove home the message that chemisorption-mediated hydrogen storage was possible in SWCNT films and technologically viable in at least some applications.

5.3. Activated carbon fibers, graphite nanofibers and intercalation compounds

Lee et al. had studied hydrogen adsorption along surface-modified ACFs in attempting to elucidate chemisorption [89].

In the samples tested, ACFs doped with Ni and F showed a consistent increase of adsorption capacity. Interestingly, a significant decrease of the micropore volume was noted in the course of doping but it was not serious enough to mask the increase of loading capacity. It has been suggested that intercalation of potassium into GNFs can augment hydrogen storage by a factor of ten, the change attributed to pore broadening. Using sophisticated simulation routines, Froudakis investigated this scenario and claimed that hydrogen adsorption had been facilitated by a charge transfer from potassium atoms to the nanotube, which gave rise to induced polarization of the hydrogen molecules by the positively charged potassium ions [19,104]. Browning et al. studied adsorption in GNFs and expressed, on the basis of kinetic data, that chemisorption was a partial contributor to the overall storage capacity and kinetics [37]. In particular, the rate-determining step leading to hydrogen storage was apparently related to hydrogen dissociation along graphitic edge sites. Such a storage mode was proposed to be consistent with chemisorption in view of the higher than expected loadings and slower kinetics compared to physisorption.

In 1987, Lagrange et al. prepared graphite intercalation compounds comprising higher-than-unity stages and heavy alkali metals [162]. The intercalated graphite structure defined a lacunar order that was able to sorb large quantities of hydrogen at temperatures close to 77 K. In the physisorbed material, the chemical formula $KC_{12s} \cdot 2H_2$ was assigned (where *s* denotes the stage). In comparison, the first-stage or stage 1 type derivative was assigned the formula $KC_8 \cdot KC_8$ was formed upon hydrogenation via chemisorptive dissociation of adsorbed dihydrogen to yield alternating planes of graphite and intercalated alkali metal layers. Indeed, a complete transformation of the solid phase structure was observed upon hydrogenation between 20 °C and 150 °C. To gain insight into the kinetics of adsorption, a mixture of protium and deuterium was loaded along the two types of intercalated materials, yielding an isotope effect. Isotopic separation was more pronounced during physisorption of KC_{24} compositions than chemisorption of KC_8 surfaces. Apart from exploiting alkali to load hydrogen into graphite compounds, other uncommon treatments such as sonication were postulated or observed to raise hydrogen adsorption [16,19,54,100,102–112].

6. Techniques used to assess hydrogen adsorption

6.1. Experimental approaches

Techniques to detect the formation of C–H bonds have been employed to probe various chemical interactions between hydrogen and carbonaceous materials. Methods to do so have included electron microscopic analysis, FT-Raman, FT-IR, XRD, X-ray photoelectron spectroscopy (XPS) and ^{13}C NMR techniques. A second requirement has been to quantify the adsorbed hydrogen per carbon atom ratio. This task has been typically achieved using atom-specific methods to probe the C1s core level carbon atoms in CNTs. With XPS, H_2 -coordination-induced chemical shifts of the C1s level have been used to identify the C–

H bonds involved. As well, the fraction of affected carbon atoms has been deduced from their relative intensities [193]. An alternative basis to study the unoccupied orbital structure has drawn upon the core excitation process of X-ray absorption spectroscopy (XAS) [194]. In particular, the formation of C–H bonds around specific carbon atoms has been inferred in the course of altering the electronic structure of a CNT.

Coming to more specific examples, several groups have obtained experimental evidence supporting the existence of chemisorbed hydrogen using sophisticated instrumental analysis techniques:

a. In 2001, low-temperature inelastic neutron scattering experiments conducted by Ren and Price revealed the influence of different adsorption sites on the strength of the hydrogen-carbon interaction in materials [195]. In particular, these findings revealed an interaction of approximately 5 kJ/mole when measured against various metal-free carbon materials [55,195]. The account concluded by confirming that surface adsorption of dihydrogen had occurred without realizing significant interaction energies, thus supporting the common belief that carbon sites alone would be too inert to activate dihydrogen. In comparison, strong interactions between dihydrogen and surface would have been expected during chemisorption. The authors argued that the hydrogen molecule must have first become activated in order to experience chemisorption, thus supporting the notion that a catalytic agent should mediate hydrogenation in carbon materials. The catalytic agent, it was professed, would be a material that would become readily coordinated to hydrogen in comparison to carbon, could aid cleavage of dihydrogen upon association and could promote transfer of hydrogen atoms to equipotential sites along the carbon surface. Surface-resident heteroatom impurities such as N, P, S and B have shown promise in this respect as hydrogen storage activators of carbonaceous materials [196]. Sankaran et al. further claimed that carbon materials contain other sites that serve to promote hydrogen adsorption and absorption [196].

b. A custom-made Sieverts apparatus has been used by Xua et al. to investigate the hydrogen storage capacity of SWNHs, SWCNTs, GNFs, ACs and graphite at room temperature and 77 K [141]. The utility of this method was made clear by its practicality. The hydrogen storage capacity of the carbon materials correlated well against their surface area, volume and average micropore diameter. In addition, the results showed that the storage capacity was less than 1 wt% at room temperature.

c. Electron microscopic analysis, FT-Raman, FT-IR, XRD, XPS and ^{13}C and ^{11}B MAS NMR techniques have all been used to investigate BCNTs. The existence of boron in different chemical environments has been confirmed by XPS and ^{11}B MAS NMR. Hydrogen absorption by such studies has yielded an apparent maximum of 2 wt% hydrogen storage capacity.

d. An atomic hydrogen beam technique [197] was employed by Nikitin et al. to monitor the facilitated hydrogenation of SWCNT films [198]. While impractical for real hydrogenation applications, the approach as a measurement technique was noteworthy in the sense that all values obtained, by default, excluded the dihydrogen dissociation component of the overall hydrogenation mechanism. XAS measurements were used to highlight a decreased π^*

character along the C=C bonds forming the walls of SWCNT films. Furthermore, XAS was used to establish an increased C–H* resonance upon hydrogenation. On the basis of XPS results combined with theoretical calculations, an approximate 65 ± 15 atom% hydrogenation of carbons was concluded to have occurred in the SWCNT films, which corresponded to 5.1 ± 1.2 wt% hydrogen capacity.

e. Micropore volume measurements have been extremely informative and are typically obtained by using several methods. With the Dubinin–Radushkevich (DR) equation, carbon dioxide adsorption data obtained at 273 K is extrapolated to quantify micropore volumes of pores ≤ 7 nm. Similarly, nitrogen adsorption data at 77 K can be used to probe the volume of pores < 2 nm. A comprehensive account of surface, volume and loading measurements has illustrated consistencies and variations between pore structure and hydrogen uptake on a variety of microporous and nanostructured carbon materials at 77 K and 1 bar pressure [6]. Among the materials chosen, surface area measurements have indicated values that ranged from modest to very high, with a maximum loading area of $2630 \text{ m}^2/\text{g}$, for instance, available along both sides of a graphene layer. Large variations in the relation between surface area and loading capacity measurements have been noted. More interestingly, some materials boasting very high total pore volume measurements did not adsorb hydrogen to a large extent at 1 bar. While perhaps counter-intuitive, the root cause of this discrepancy could be narrowed, thanks to this technique, to the much smaller interaction energy of hydrogen in wide pores compared to small micropores (< 0.7 nm). Furthermore, the correlation of measured data points showed greater scattering for surface areas exceeding $1000 \text{ m}^2/\text{g}$. This aspect was likely related to the wider pore size distributions often found in materials possessing larger surface areas. That being said, measurement techniques may also be prone to error, and materials demonstrating high apparent surface areas have often manifested erroneous contributions from pore filling effects.

f. XPS has been used by Ruffieux et al. to probe the interaction of dihydrogen with sp^2 -hybridized carbons on graphite (0001), SWCNTs and C60 multilayer films [199]. These substrates were chosen to sample the diverse range of curvatures representative of the established classes of carbon networks. XPS spectroscopy of samples treated with atomic hydrogen and low-energy hydrogen ions revealed that hydrogen had been chemisorbed along the basal plane of sp^2 -bonded carbon networks, as evidenced by the reduced emission from π -derived states and a reduction of the electron work function by as much as 1.3 eV. The kinetic energy barrier to hydrogen adsorption was determined to be strongly curvature-dependent. Indeed, activation energies were observed to decrease as local curvatures increased along the carbon network. In the case of C60 and single-walled carbon nanotubes, hydrogen chemisorption was validated upon exposure to atomic hydrogen. In contrast, chemisorption on graphite (0001) was promoted by hydrogen ions of low kinetic energy (~ 1 eV). Not surprisingly, the energy barrier to subsequent adsorption events was shown to incrementally increase upon progressive hydrogen saturation. Apart from XPS measurements, scanning tunneling microscopy of individual adsorption sites on a graphite (0001) surface revealed

long-range (~5 nm) electronic effects. It seemed that the superstructure had originated from the scattering of delocalized electronic wave functions at point defects. The resultant standing waves, in turn, had induced a redistribution of the local density of states.

g. A near edge X-ray absorption spectroscopy (NEXAFS)-based method was developed in 2005 by Lenardi et al. to quantitatively evaluate the chemisorbed fraction of hydrogen in nanostructured carbon films [200]. In the carbon K-edge spectrum obtained, the peak identifying the C–H carbons was assumed to directly reflect the amount of hydrogen bonded to carbon. The assumption was supported by a comparative analysis of gas-phase hydrocarbons examined via electron energy loss spectroscopy (EELS). The NEXAFS method was subsequently applied to the analysis of nanostructured carbon films synthesized via supersonic cluster beam deposition. Following exposure to molecular hydrogen (0.12 MPa, 3 h, room temperature), various samples yielded a hydrogen loading of approximately ~1.5 wt%.

h. Imamura et al. used thermal desorption spectrometry (TDS) and neutron diffraction measurements to characterize the hydrogen loading of certain carbon nanocomposites. The materials, which were prepared by ball milling graphite, magnesium and benzene or cyclohexane under various conditions, displayed novel hydrogen storage traits [201]. The measurement techniques established in particular that hydrogen uptake had proceeded by at least two mechanisms. In the simplest sense, some hydrogens had become strongly associated to the carbon component whereas the remaining were held as hydrides in the magnesium component. The findings were particularly interesting, as ball milling had generated large amounts of dangling carbon bonds in the graphite substrate. These “loose ends” served as active sites in the uptake of hydrogen. When hydrogenated composites were incubated with deuterium gas at 453 K, deuterium exchange was found to occur with the magnesium hydride component, but not with any hydrogen directly associated to the carbon.

i. Nitrogen physisorption, X-ray diffraction, transmission electron microscopy, metal surface area analysis, and temperature-programmed hydrogen reduction and desorption methods have been used by Zieliński et al. to characterize hydrogen storage in a nickel-doped commercially activated carbon source [202]. Furthermore, a high-pressure volumetric adsorption–desorption system was used to measure hydrogen storage and release at room temperature and 20–30 bar. A variety of parameters such as the metal type, metal content and preparation history were examined in view of their established influence on hydrogen uptake. Overall, stored hydrogen was deemed to have been loosely chemisorbed along the carbonaceous material. More interestingly, hydrogen seemed to have chemisorbed to carbon acceptor sites, which had been induced by H₂-pretreatment at 623 K.

6.2. Theoretical approaches

Complicated model systems notwithstanding, theoretical approaches have proven extremely convenient and supportive in validating and better directing the development of hydrogen storage media. In as much that CNTs feature well-defined structures, most work on carbonaceous storage

media has necessarily focused on these carbon allotropes and their metal-doped variants. The density functional theory and several universal force field models have proven very useful in modeling CNT hydrogenation as a function of heteroatom substitution and location. By way of these techniques, hydrogenation activators such as nitrogen, phosphorus, sulfur and boron have been compared and their optimal placement along various carbon surfaces has been predicted. This contribution has served particularly well in providing a rational basis to target the most suitable chemical activators, geometries and related design requirements in efforts to yield CNTs with high storage capacities [196]. Using density functional theory, Chen et al. systematically assessed the potential mechanisms of hydrogen spill-over into several carbon-based materials [190]. Modeled in particular was the adsorption and diffusion of atomic hydrogen in graphene sheets, SWCNTs and hexabenzocoronene. Furthermore, the minimum-energy-pathway potential energy maps of selected adsorption and diffusion scenarios could be modeled. In this treatment, the migration of atomic hydrogen from the Pt cluster to the substrate was shown to easily proceed at ambient conditions. While slightly endothermic, indicative of adsorption along carbon, the simulation nonetheless revealed a small kinetic energy barrier. The results also affirmed that diffusion of carbon-chemisorbed hydrogen atoms would be energetically prohibited, as any such migration would require rupture of the C–H bond. Hence, the findings implied that hydrogen spill-over would likely occur via a physisorption mode. Also, the mobility of H atoms was found to reflect the surface curvature of carbon.

In a related study, Lueking and Yang [191] systematically addressed the hydrogen storage issue and confirmed that hydrogen storage in various carbon-catalyst materials could be increased via hydrogen spill-over from a supported catalyst. In particular, the group illustrated that a dynamic steady-state model was needed to predict the nature of hydrogen spill-over. The work focused on secondary spill-over experiments to bypass unpredictable events associated with primary spill-over, such as sporadic material changes.

7. Conclusion

As hydrogen storage describes one of the key challenges in developing a clean-burning hydrogen economy, it is not surprising that much effort has focused on optimizing the current state of storage technologies. In keeping with this theme, nanostructured carbon materials do indeed feature commercial advantages over other storage methods. As well, they boast flexibilities relating to their design and the choice to employ physical and/or combined physicochemical storage strategies. Some nanostructured carbon storage materials, particularly microporous carbons and CNTs, are currently depicted as the best hydrogen storage media in light of their improved capacities, favorable kinetic behavior, and moderately good reproducibility and self-consistency amongst differing experimental and theoretical test methods. That being said, several isolated accounts depicting the tremendous potential of GNFs should not be regarded lightly, as it is possible that further development and clarification of the

microscopic storage mode could propel GNFs into the limelight.

Despite all the encouraging developments, current nano-material technologies still remain far from meeting the DOE target of 6.5 wt% loaded hydrogen. While hydrogen storage capacities and kinetics have been satisfactorily quantified in carbonaceous materials, the mechanisms of hydrogen uptake and release remain to be better elucidated. Preparing future designs for hydrogen storage appears to rest upon better understanding many factors such as the nature of the surface-dependent functional groups, the pore and surface microstructure and topology, the adsorption and desorption properties, the thermodynamic and kinetic behavior of pure materials as well as their metal-doped composites, and the hydrogen uptake–release mechanism. It follows that a most crucial technical target is to optimize the adsorption sites of the carbon network and thereby to facilitate the kinetics of loading and release, particularly under room temperature and moderate pressure conditions. Such an undertaking will also require a precise knowledge of the interaction between hydrogen and a given carbon surface, as many examples herein have exemplified interactions and mechanisms that were physical, chemical or possibly intermediate. Clearly, if nanostructured carbons are to become the base materials of a hydrogen-storage technology, many improvements remain to be achieved. This goal can be released by identifying and characterizing all physicochemical contributors to the overall problem and systematically optimizing each one.

REFERENCES

- [1] Sandrock G. Application of hydrides. In: Yürüm Y, editor. Hydrogen energy system. NATO ASI Series, E: Applied sciences, vol. 295. Dordrecht: Kluwer Academic Publishers; 1995. p. 253–80.
- [2] Sandrock G. Hydrogen–metal systems. In: Yürüm Y, editor. Hydrogen energy system. NATO ASI Series, E: Applied sciences, vol. 295. Dordrecht: Kluwer Academic Publishers; 1995. p. 135–66.
- [3] Züttel A. Mater Today 2003;6:24–33.
- [4] Grochala W, Edwards PP. Chem Rev 2004;104:1283–316.
- [5] Bogdanovic B, Schwickardi M. J Alloys Compd 1997;253:254–1–9.
- [6] Thomas KM. Catalysis Today 2007;120:389–98.
- [7] Chambers A, Parks C, Baker RTK, Rodriguez NM. J Phys Chem B 1998;102:4253–6.
- [8] Dillon AC, Jones KM, Bekkedahl TA, Kiang CH, Bethune DS, Heben MJ. Nature 1997;386:377–9.
- [9] Liu C, Fan YY, Liu M, Cong HT, Cheng HM, Dresselhaus MS. Science 1999;286:1127–9.
- [10] Lee SM, Park KS, Choi YC, Park YS, Bok JM, Bae DJ. Synth Met 2000;113:209–16.
- [11] Ye Y, Ahn CC, Witham C, Fultz B, Liu J, Rinzler AG. Appl Phys Lett 1999;74:2307–9.
- [12] Lueking A, Yang RT. J Catal 2002;206:165–8.
- [13] Chen P, Wu X, Lin J, Tan KL. Science 1999;285:91–3.
- [14] Pinkerton FE, Wicke BG, Olk CH, Tibbetts GG, Meisner GP, Meyer MS. J Phys Chem B 2000;104:9460–7.
- [15] Yang RT. Carbon 2000;38:623–6.
- [16] Wang Q, Johnson JK. J Phys Chem B 1999;103:4809–13.
- [17] Dodziuk H, Dolgonos G. Chem Phys Lett 2002;356:79–83.
- [18] Lee SM, Lee YH. Appl Phys Lett 2000;76:2877–9.
- [19] Froudakis GE. Nano Lett 2001;1:179–82.
- [20] Berry GD, Aceves SM. Energy Fuels 1998;12:49–55.
- [21] Seayad AM, Antonelli DM. Adv Mater 2004;16:765–77.
- [22] Schlapbach L, Züttel A. Nature 2001;414(6861):353–8.
- [23] Dillon AC, Heben MJ. Appl Phys A Mater Sci Process 2001;72:133–42.
- [24] Anson A, Callejas MA, Benito AM, Maser WK, Izquierdo MT, Rubio B. Carbon 2004;42:1243–8.
- [25] Challet S, Azais P, Pellenq RJM, Isnard O, Soubeyroux JL, Duclaux L. J Phys Chem Solids 2004;65:541–4.
- [26] Li XS, Zhu HW, Ci LJ, Xu CL, Mao ZQ, Wei BQ. Carbon 2001;39:2077–9.
- [27] Hwang JY, Lee SH, Sim KS, Kim JW. Synth Metals 2002;126:81–5.
- [28] Lupu D, Biris AR, Misan I, Jianu A, Holzhuber G, Burkel E. Int J Hydrogen Energy 2004;29:97–102.
- [29] Shaijumon MM, Ramaprabhu S. Int J Hydrogen Energy 2005;30:311–7.
- [30] Ci LJ, Zhu HW, Wei BQ, Xu CL, Wu DH. Appl Surf Sci 2003;205:39–43.
- [31] Callejas MA, Anson A, Benito AM, Maser W, Fierro JLG, Sanjuan ML. Mater Sci Eng B Solid State Mater Adv Technol 2004;108:120–3.
- [32] Huang WZ, Zhang XB, Tu JP, Kong FZ, Ma JX, Liu F. Mater Chem Phys 2003;78:144–8.
- [33] Zhu HW, Li CH, Li XS, Xu CL, Mao ZQ, Liang J. Mater Lett 2002;57:32–5.
- [34] Hou PX, Xu ST, Ying Z, Yang QH, Liu C, Cheng HM. Carbon 2003;41:2471–6.
- [35] Cheng HM, Liu C, Fan YY, Li F, Su G, Cong HT. Zeitschrift fur Metallkunde 2000;91:306–10.
- [36] Zhu HW, Chen A, Mao ZQ, Xu CL, Xiao X, Wei BQ. J Mater Sci Lett 2000;19:1237–9.
- [37] Browning DJ, Gerrard ML, Lakeman JB, Mellor IM, Mortimer RJ, Turpin MC. Nano Lett 2002;2:201–5.
- [38] Bai XD, Zhong DY, Zhang GY, Ma XC, Liu S, Wang EG. Appl Phys Lett 2001;79:1552–4.
- [39] Wang QK, Zhu CC, Liu WH, Wu T. Int J Hydrogen Energy 2002;27:497–500.
- [40] Gupta BK, Srivastava ON. Int J Hydrogen Energy 2000;25:825–30.
- [41] Fan YY, Liao B, Liu M, Wei YL, Lu MQ, Cheng HM. Carbon 1999;37:1649–52.
- [42] Gupta BK, Tiwari RS, Srivastava ON. J Alloys Compd 2004;381:301–8.
- [43] Nijkamp MG, Raaymakers JEMJ, van Dillen AJ, de Jong KP. Appl Phys A Mater Sci Process 2001;72:619–23.
- [44] Takagi H, Hatori H, Soneda Y, Yoshizawa N, Yamada Y. Mater Sci Eng B Solid State Mater Adv Technol 2004;108:143–7.
- [45] Zhao XB, Xiao B, Fletcher AJ, Thomas KM. J Phys Chem B 2005;109:8880–8.
- [46] Zhao XB, Villar-Rodil S, Fletcher AJ, Thomas KM. J Phys Chem B 2006;110:9947–55.
- [47] Schimmel HG, Nijkamp G, Kearley GJ, Rivera A, de Jong KP, Mulder FM. Mater Sci Eng B 2004;108:124–9.
- [48] Schimmel HG, Kearley GJ, Nijkamp MG, Visser CT, de Jong KP, Mulder FM. Chem Eur J 2003;9:4764–70.
- [49] Texier-Mandoki N, Dentzer J, Piquero T, Saadallah S, David PC, Vix-Guterl C. Carbon 2004;42:2744–7.
- [50] Panella B, Hirscher M, Roth S. Carbon 2005;43:2209–14.
- [51] Benard P, Chahine R. Langmuir 2001;17:1950–5.
- [52] Poirier E, Chahine R, Tessier A, Bose TK. Rev Sci Inst 2005;76:55101–6.
- [53] Gundiah G, Govindaraj A, Rajalakshmi N, Dhathathreyan KS, Rao CNR. J Mater Chem 2003;13:209–13.
- [54] Zhou Y, Feng K, Sun Y, Zhou L. Chem Phys Lett 2003;380:526–9.

- [55] Shiraishi M, Takenobu T, Kataura H, Ata M. *Appl Phys A* 2004;78:947–53.
- [56] Takagi H, Hatori H, Yamada Y, Matsuo S, Shiraishi M. *J Alloys Compd* 2004;385:257–63.
- [57] Kayiran SB, Lamari FD, Levesque D. *J Phys Chem B* 2004;108:15211–5.
- [58] Gadiou R, Saadallah S, Piquero T, David P, Parmentier J, Vix-Guterl C. *Mic Mes Mater* 2005;79:121–8.
- [59] Pang J, Hampsey JE, Wu Z, Hu Q, Lu Y. *Appl Phys Lett* 2004;85:4887–9.
- [60] Takagi H, Hatori H, Soneda Y, Yoshizawa N, Yamada Y. *Mater Sci Eng B* 2004;108:143–7.
- [61] Zhou L, Zhou Y, Sun Y. *Int J Hydrogen Energy* 2004;29:475–9.
- [62] Parra JB, Ania CO, Arenillas A, Rubiera F, Palacios JM, Pis JJ. *J Alloys Compd* 2004;379:280–9.
- [63] Gogotsi Y, Dash RK, Yushin G, Yildirim T, Laudisio G, Fischer JE. *J Am Chem Soc* 2005;127:16006–7.
- [64] Hynek S, Fuller W, Bentley J. *Int. J. Hydrogen Energy* 1997;22:601–10.
- [65] Zijlstra H, Westendorp FF. *Solid State Commun* 1969;7:857–9.
- [66] van Vucht JHN, Kuijpers FA, Bruning HCAM. *Philips Res Rep* 1970;25:133–46.
- [67] Li Y, Zhao D, Wang Y, Xue R, Shen Z, Li X. *Int J Hydrogen Energy* 2006;32:2513–7.
- [68] Jin H, Lee YS, Hong I. *Catalysis Today* 2007;120:399–406.
- [69] Bénard P, Chahine R. *Scripta Materialia* 2007;56:803–8.
- [70] Gardiner M, Bradley K. National Hydrogen Association's 14th annual US Hydrogen Conference, Washington, DC, March 6, 2004.
- [71] Lee EY, Suh MP. *Angew Chem Int Ed* 2004;43:2798.
- [72] Chen B, Ockwig NW, Millward AR, Contreras DS, Yaghi OM. *Angew Chem Int Ed* 2005;44:4745.
- [73] Foster PM, Eckert J, Chang J-S, Park S-E, Ferey G, Cheetham AK. *J Am Chem Soc* 2003;125:1309.
- [74] Bogdanovic B, Felderhoff M, Kaskel S, Pommerin A, Schlichte K, Schuth F. *Adv Mater* 2003;15:1012–5.
- [75] Rosi NL, Eckert J, Eddaoudi M, Vodak DT, Kim J, O'Keefe M. *Science* 2003;300:1127–9.
- [76] Ma RZ, Bando Y, Zhu HW, Sato T, Xu CL, Wu DH. *J Am Chem Soc* 2002;124:7672–3.
- [77] Chen P, Xiong ZT, Luo JZ, Lin JY, Tan KL. *Nature* 2002;420:302–4.
- [78] Shao HY, Xu HR, Wang YW, Li XG. *Nanotechnology* 2004;15:269–74.
- [79] Tibbetts GG, Meisner GP, Olk CH. *Carbon* 2001;39:2291–301.
- [80] Ritschel M, Uhlemann M, Gutfleisch O, Leonhardt A, Graff A, Taschner C. *Appl Phys Lett* 2002;80:2985–7.
- [81] Cheng HM, Yang QH, Liu C. *Carbon* 2001;39:1447–54.
- [82] Bauqman RH, Zakhidov AA, de Heer WA. *Science* 2002;297:787–92.
- [83] Cao D, Feng P, Wu J. *Nano Lett* 2004;4:1489–92.
- [84] Wang Q, Johnson JK. *J Phys Chem B* 1999;103:277–81.
- [85] Heine T, Zhechkov L, Seifert G. *Phys Chem Chem Phys* 2004;6:980–4.
- [86] Zhou L, Zhang JS, Zhou YP. *Langmuir* 2001;17:5503–7.
- [87] Georgiev PA, Ross DK, Albers P, Ramirez-Cuesta AJ. *Carbon* 2006;44:2724–38.
- [88] Sankaran M, Viswanathan B. *Carbon* 2006;44:2816–21.
- [89] Lee YS, Kim YH, Hong JS, Suh JK, Cho GJ. *Catal Today* 2007;120:420–5.
- [90] Bhatia SK, Myers AL. *Langmuir* 2006;22:1688–700.
- [91] Ye X, Gu X, Gong XG, Shing TKM, Liu ZF. *Carbon* 2007;45:315–20.
- [92] (a)Georgakis M, Stavropoulos G, Sakellaropoulos GP. *Int J Hydrogen Energy* 2007;32:1999–2004;
(b)Georgakis M, Stavropoulos G, Sakellaropoulos GP. *Int J Hydrogen Energy* 2007;32:3465–70.
- [93] Lee H, Kang Y-S, Kim S-H, Lee J-Y. *Appl Phys Lett* 2002;80:577–9.
- [94] Lueking A, Yang RT. *AIChE J* 2003;49:1556–68.
- [95] Hou P-X, Yang Q-H, Bai S, Xu S-T, Liu M, Cheng H-M. *J Phys Chem B* 2002;106:963–6.
- [96] Shiraishi M, Takenobu T, Ata M. *Chem Phys Lett* 2003;367:633–6.
- [97] Kelly KF, Chiang IW, Mickelson ET, Hauge RH, Margrave JL, Wang X, et al. *Chem Phys Lett* 1999;313:445–50.
- [98] Kuznetsova A, Mawhinney DB, Naumenko V, Yates Jr JT, Liu J, Smalley RE. *Chem Phys Lett* 2000;321:292–6.
- [99] Brown CM, Yildirim T, Neumann DA, Heben MJ, Gennett T, Dillon AC, et al. *Chem Phys Lett* 2000;329:311–6.
- [100] Hirscher M, Becher M, Haluska M, Dettlaff-Weglikowska U, Quintel A, Duesberg GS. *Appl Phys A* 2001;72:129–32.
- [101] Cao A, Zhu H, Zhang X, Li X, Ruan D, Xu C, et al. *Chem Phys Lett* 2001;342:510–4.
- [102] Ding RG, Lu GQ, Yan ZF, Wilson MA. *J Nanosci Nanotechnol* 2001;1:7–29.
- [103] Nijkamp MG. Inorganic chemistry and catalysis. PhD thesis, Debye Institute, Utrecht University, The Netherlands; 2002.
- [104] Froudakis GE. *Nano Lett* 2001;1:531–3.
- [105] Wang K, Johnson JK. *Mol Phys* 1998;95:299–309.
- [106] Wang K, Johnson JK. *J Chem Phys* 1999;110:577–86.
- [107] Simonyan VV, Diep P, Johnson JK. *J Chem Phys* 1999;111:9778–83.
- [108] Darkrim F, Levesque D. *J Chem Phys* 1998;109:4981–4.
- [109] Rzepka M, Lamp P, de la Casa-Lillo MA. *J Phys Chem B* 1998;102:10894–8.
- [110] Gordon PA, Saeger RB. *Ind Eng Chem Res* 1999;38:4647–55.
- [111] Yin YF, Mays T, McEnaney B. *Langmuir* 2000;16:10521–7.
- [112] Cheng HS, Pez G, Kern G, Kresse G, Hafner J. *J Phys Chem B* 2001;105:736–42.
- [113] Claye A, Fischer JE. *Electrochim Acta* 1999;45:107–20.
- [114] Zhou L. *Renewable Sustainable Energy Rev* 2005;9:395–408.
- [115] Chen GX, Hong MH, Ong TS, Lam HM, Chen WZ, Elim HI, et al. *Carbon* 2004;42:2735–7.
- [116] Touzik A, Hermann H. *Chem Phys Lett* 2005;416:137–41.
- [117] Zhan L, Li K, Zhu X, Lv C, Ling L. *Carbon* 2002;40:455–7.
- [118] Iijima S. *Nature* 1991;354:56–8.
- [119] Shiraishi M, Takenobu T, Yamada A, Ata M, Kataura H. *Chem Phys Lett* 2002;358:213–8.
- [120] Zhang C, Lu X, Gu A. *Int J Hydrogen Energy* 2004;29:1271–6.
- [121] Wu XB, Chen P, Lin J, Tan KL. *Int J Hydrogen Energy* 2000;25:261–5.
- [122] Johansson E, Hjärvärsson B, Ekström T, Jacob M. *J Alloys Compd* 2002;330–332:670–5.
- [123] Züttel A, Nützenadel Ch, Sudan P, Mauron Ph, Emmenegger Ch, Rentsch S, et al. *J Alloys Compd* 2002;330–332:676–82.
- [124] Zheng Q, Gu A, Lu X, Lin W. *Int J Hydrogen Energy* 2004;29:481–9.
- [125] Gupta BK, Srivastava ON. *Int J Hydrogen Energy* 2001;26:857–62.
- [126] Ahn CC, Ye Y, Ratnakumar BV, Witham C, Bowman Jr RC, Fultz B. *Appl Phys Lett* 1998;73(23):3378–80.
- [127] Schur DV, Tarasov BP, Zaginaichenko SYu, Pishuk VK, Veziroglu TN, Shul'ga YM. *Int J Hydrogen Energy* 2002;27:1063–9.
- [128] Kiyobayashi T, Takeshita HT, Tanaka H, Takeichi N, Züttel A, Schlapbach L. *J Alloys Compd* 2002;330–332:666–9.
- [129] Zhou L, Zhou Y, Sun Y. *Int J Hydrogen Energy* 2004;29:319–22.
- [130] Pradhan BK, Harutyunyan A, Stojkovic D, Zhang P, Cole MW, Crespi V. Marine research society symposium proceedings, In: Bernier P, Ajayan P, Iwasa Y, Nikolaev P, editors. Making functional materials with nanotubes, vol. 706; 2002. p. Z10.3.

- [131] Chen X, Dettlaff-Weglikowska U, Haluska M, Hulman M, Roth S, Hirscher M. Making functional materials with nanotubes. In: Bernier P, Ajayan P, Iwasa Y, Nikolaev P, editors. Marine research society symposium proceedings, vol. 706; 2002. p. Z10.3.
- [132] Furuya Y, Hashishin T, Iwanaga H, Motojima S, Hishikawa Y. Carbon 2004;42:331–5.
- [133] Liu F, Zhang X, Cheng J, Tu J, Kong F, Huang W, et al. Carbon 2003;41:2527–32.
- [134] Sumanasekera GU, Adu CKW, Pradhan BK, Chen G, Romero HE, Eklund PC. Marine research society symposium proceedings, In: Bernier P, Ajayan P, Iwasa Y, Nikolaev P, editors. Making functional materials with nanotubes, vol. 706; 2002. p. Z10.4.
- [135] Cheng J, Yuan X, Zhao L, Huang D, Zhao M, Dai L, Ding R. Carbon 2004;42:2019–24.
- [136] Guay P, Stansfield BL, Rochefort A. Carbon 2004;42:2187–93.
- [137] Mpourmpakis G, Froudakis GE, Lithoxoos GP, Samios J. Nano Lett 2006;6:1581.
- [138] Takagi H, Hattori H, Soneda Y, Yoshizawa N, Yamada Y. Mater Sci Eng B 2004;108:143–7.
- [139] de la Casa-Lillo MA, Lamari-Darkrim F, Cazorla-Amoros D, Linares-Solano A. J Phys Chem B 2002;106:10930–4.
- [140] Frankland SJV, Brenner DW. Chem Phys Lett 2001;344:18.
- [141] Xu WC, Takahashi K, Matsuo Y, Hattori Y, Kumagai M, Ishiyama S, et al. Int J Hydrogen Energy 2007;32:2504–12.
- [142] Texier-Mandoki N, Dentzer J, Piquero T, Saadallah S, David P, Vix-Guterl C. Carbon 2004;42:2735–77.
- [143] Yildirim T, Ciraci S. Phys Rev Lett 2005;94. 175501–1-4.
- [144] Lee JW, Kim HS, Lee JY, Kang JK. Appl Phys Lett 2006;88. 143126–1-30.
- [145] Yildirim T, Íñiguez J, Ciraci S. Phys Rev B 2005;72. 153403–1-4.
- [146] Luxembourg D, Flamant G, Bêche E, Sans JL, Giral J, Goetz V. Int J Hydrogen Energy 2007;32:1016–23.
- [147] Bansal RC, Donet J-P, Stoeckli F. Active carbon. New York: Marcel Dekker; 1988.
- [148] Dobruskin VKh. Carbon 2002;40:659–66.
- [149] Suzuki T, Kaneko K, Setoyama N, Maddox M, Gubbins K. Carbon 1996;34:909–12.
- [150] Yins YF, McEnaney B, Mays TJ. Carbon 1998;36:1425–32.
- [151] Okayama T, Yoneya J, Nitta T. Fluid Phase Equilibria 1995; 104:305–16.
- [152] Jagiello J, Thommes M. Carbon 2004;42:1227–32.
- [153] Do DD, Do HD. Langmuir 2004;20:7103–16.
- [154] Bhatia SK, Tran K, Nguyen TX, Nicholson D. Langmuir 2004; 20:9612–20.
- [155] Biggs MJ, Buts A, Williamson D. Langmuir 2004;20:5786–800.
- [156] Jeloica L, Sidis V. Chem Phys Lett 1999;300:157–62.
- [157] Breck DW, Grose RW. In: Meier WM, Uytterhoeven JB, editors. Molecular sieves, vol. 319. Washington, DC: American Chemical Society; 1973.
- [158] Goulay AM, Tsakiris J, Cohen de Lara E. Langmuir 1996;12:371–8.
- [159] Klein J, Kumacheva E. Science 1995;269:816–20.
- [160] Carrott PJM, Roberts RA, Sing KSW. A new method for the determination of micropore size distribution. In: Unger KK, Rouquerol J, Sing KSW, Kral H, editors. Characterization of porous solids, vol. 89. Amsterdam, The Netherlands: Elsevier; 1988.
- [161] Rud AD, Lakhnik AM, Ivanchenko VG, Uvarov VN, Shkola AA, Dekhtyarenko VA, et al. Int J Hydrogen Energy 2008;33:1310–6.
- [162] Lagrange P, Guerard D, Mareche JF, Herold A. J Less Common Metals 1987;131:371–8.
- [163] Hirscher M, Becher M, Haluska M, Quintel A, Skakalova V, Choi Y-M. J Alloys Compd 2002;330–332:654–8.
- [164] Simonyan VV, Johnson JK. J Alloys Compd 2002;330–332:659–65.
- [165] Dresselhaus MS, Willianms KA, Eklund PC. MRS Bull 1999; Nov:45–50.
- [166] Takagi H. J Japan Inst Energy 2002;81(10):891–7.
- [167] Iijima S, Yudasaka M, Yamada R, Bandow S, Suenaga K, Kokai F. Chem Phys Lett 1999;309:165–70.
- [168] Agarwal RK, Noh JS, Schwarz JA, Davini P. Carbon 1987;25: 219–26.
- [169] Pacula A, Mokaya R. J Phys Chem C 2008;112:2764–9.
- [170] Dag S, Ozturk Y, Ciraci S, Yildirim T. Phys Rev B 2005;72: 155404–8.
- [171] Zhao Y, Kim YH, Dillon AC, Heben MJ, Zhang SB. Phys Rev Lett 2005;94:155504.
- [172] Kubas GJ, Ryan RR, Swanson BI, Vergamini PJ, Wasserman HJ. J Am Chem Soc 1984;106:451–2.
- [173] Kubas GJ. J Organomet Chem 2001;635:37–68.
- [174] Zacharia R, Rather S, Hwang SW, Nahm KS. Chem Phys Lett 2007;434:286–91.
- [175] Yang FH, Lachawiec AJ, Yang RT. J Phys Chem B 2006;110:6236–44.
- [176] Zacharia R, Rather S, Hwang SW, Stephan AM, Nahm KS. In: Nathan A, Amaratunga G, Nookala M, Scanlon LG, Morinobu E, editors. Mobile energy. Mater Res Soc Symp Proc 973E. Warrendale, PA; 2007.
- [177] Anón A, Lafuente E, Urriolabeitia E, Navarro R, Benito AM, Maser WK, et al. J Phys Chem B 2006;110:6643–8.
- [178] Sankaran M, Viswanathan B. Carbon 2007;45:1628–35.
- [179] Leela Mohana Reddy A, Ramaprabhu S. Int J Hydrogen Energy 2008;33:1028–34.
- [180] Zacharia R, Kim KY, Kibria AKMF, Nahm KS. Chem Phys Lett 2005;412:369–75.
- [181] Rather S, Zacharia R, Hwang SW, Naik M, Nahm KS. Chem Phys Lett 2007;441:261–7.
- [182] Campesi R, Cuevas F, Gadiou R, Leroy E, Hirscher M, Vix-Guterl C, et al. Carbon 2008;46:206–14.
- [183] Ryoo R, Joo SH, Jun S. J Phys Chem B 1999;103:7743–6.
- [184] Schüth F. Angew Chem Int Ed 2003;42:3604–22.
- [185] Lee J, Han S, Hyeon T. J Mater Chem 2004;14:478–86.
- [186] Sakintuna B, Yürüm Y. Ind Eng Chem Res 2005;44:2893–902.
- [187] Gadiou R, Vix-Guterl C. Ann Chim Sci Mater 2005;30:425–39.
- [188] Sakintuna B, Yürüm Y. Mic Mes Mat 2006;93:304–12.
- [189] Lu AH, Schüth F. Adv Mater 2006;18:1793–805.
- [190] (a) Chen L, Cooper AC, Pez GP, Cheng H. J Phys Chem C 2007; 111:5514–9;
(b) Chen L, Cooper AC, Pez GP, Cheng H. J Phys Chem C 2007; 111:18995–9000.
- [191] Lueking AD, Yang RT. Appl Cat A: General 2004;265:259–68.
- [192] McDaniel FD, Naab FU, Holland OW, Dhoubhadel M, Mitchell LJ, Duggan JL. Surf Coat Technol 2007;201:8564–7.
- [193] Nilsson A. J Electron Spectrosc Relat Phenom 2002;126:3–42.
- [194] Stohr J. NEXAFS spectroscopy. Berlin: Springer; 1996.
- [195] Ren Y, Price DL. Appl Phys Lett 2001;79:3684–6.
- [196] Sankaran M, Viswanathan B, Srinivasa S. Int J Hydrogen Energy 2008;33:393–403.
- [197] Nikitin A, Ogasawara H, Mann D, Denecke R, Zhang Z, Dai H, et al. Phys Rev Lett 2005;95. 225507–1-4.
- [198] Ruffieux P, Gröning O, Biemann M, Mauron P, Schlapbach L, Gröning P. Phys Rev B 2002;66:245416–8.
- [199] Ruffieux P, Gröning O, Biemann M, Mauron P, Gröning P. Appl Phys A Mater Sci Process 2004;78:975–80.
- [200] Lenardi C, Marino M, Barborini E, Piseri P, Milani P. Eur Phys J B 2005;46:441–7.
- [201] Imamura H, Kitazawa I, Tanabe Y, Sakata Y. Int J Hydrogen Energy 2007;32:2408–11.
- [202] Zieliński M, Wojcieszak R, Monteverdi S, Mercy M, Bettahar MM. Int J Hydrogen Energy 2007;32:1024–32.